Non-universal behavior of leaky surface waves in a one dimensional asymmetric plasmonic grating

Sesha Vempati, Tahir Iqbal, and Sumera Afsheen

Citation: Journal of Applied Physics **118**, 043103 (2015);
View online: https://doi.org/10.1063/1.4927269
View Table of Contents: http://aip.scitation.org/toc/jap/118/4
Published by the American Institute of Physics

Non-universal behavior of leaky surface waves in a one dimensional asymmetric plasmonic grating

Sesha Vempati,[1,a),b)] Tahir Iqbal,[2,a),b)] and Sumera Afsheen[3]
[1]*UNAM-National Nanotechnology Research Center, Bilkent University, Ankara 06800, Turkey*
[2]*Department of Physics, Institute of Natural Sciences, University of Gujrat, Hafiz Hayat Campus, Gujrat 50700, Pakistan*
[3]*Department of Zoology, Institute of Life Sciences, University of Gujrat, Hafiz Hayat Campus, Gujrat 50700, Pakistan*

(Received 6 May 2015; accepted 10 July 2015; published online 22 July 2015)

We report on a non-universal behavior of leaky surface plasmon waves on asymmetric (Si/Au/analyte of different height) 1D grating through numerical modelling. The occurrence of the leaky surface wave was maximized (suppressing the Fabry–Perot cavity mode), which can be identified in a reflection spectrum through characteristic minimum. Beyond a specific analyte height (h), new sets of surface waves emerge, each bearing a unique reflection minimum. Furthermore, all of these minima depicted a red-shift before saturating at higher h values. This saturation is found to be non-universal despite the close association with their origin (being leaky surface waves). This behavior is attributed to the fundamental nature and the origin of the each set. Additionally, all of the surface wave modes co-exit at relatively higher h values. © *2015 AIP Publishing LLC*.
[http://dx.doi.org/10.1063/1.4927269]

INTRODUCTION

From early 1980s,[1,2] surface plasmon[3,4] based optical sensors have been exhibiting a great potential in evaluating physical, chemical, and biological parameters.[5–9] These sensors are 1D or 2D gratings[5,10–14] apart from gold colloids/its variations,[6,15] ring resonators,[8,16] evanescent field optical waveguides,[17] etc. These applications are dependent on the sensitivity of surface plasmon polaritons (SPPs) to the refractive index (RI) of the medium adjacent to the metal surface.[3,4,13,18] Among the various types, grating structure can be compact and robust, which are desirable characteristics for integration into other devices[6] apart from the tunability of the spectral response through geometrical parameters.[10–12,19–21] Especially, 1D grating can support waveguide, propagating SPPs and/or surface wave modes.[10,14,19] The grating parameters can be tuned to maximize any of the above modes, which may be featured in the optical properties. In the present report, we limit our interest to the asymmetric grating,[22] which supports leaky surface waves predominantly. The asymmetric grating depicts minima in the reflection spectrum corresponding to the SPPs due to the interaction between longitudinal and transverse resonant modes.[10,19,23] The applications of gratings are not limited to the detection of RI,[5,10–13,18] but extends to the estimation of analyte height (h)[10,24] where the latter is quite interesting, and the least explored as far as we can ascertain. In the context of detection of h, the spectral shift of surface wave resonance can be quantified, similar to that of RI. Notably, in an earlier study,[10] the detection of "h" is investigated, however, up to a maximum of 500 nm for a specific design employing predominantly surface waves. Importantly, beyond the above mentioned h value, some key observations were made, *viz.*, (a) the spectral shift of the minimum that corresponds to the surface wave saturates after a certain h, (b) because of the changes in the effective RI (increasing h value) additional sets ($\geq$3) of surface waves emerge, and (c) the new sets exhibit saturation behavior with increasing h, however qualitatively not similar to the earlier occurred set.

In this report, finite element method is adopted to analyze the behavior of the surface waves of Au grating on Si substrate. The grating parameters were optimized[10,19] to maximize the absorption of propagating SPPs (surface wave). The spectral shift for each set of surface wave is pursued for various h values. The non-universal behavior of the saturation with respect to h is interpreted based on the origin and fundamental nature of the each set of surface wave.

GRATING STRUCTURE AND COMPUTATIONAL DETAILS

Fig. 1(a) shows the schematic of a 1D Au grating on Si-substrate, where Λ—periodicity, t—thickness, a—slit width, and h—analyte height for a fixed RI of 1.33. The source-field is a plane wave of TM-polarization (two in plane field components E_x and E_y, whereas H_z orthogonal to the

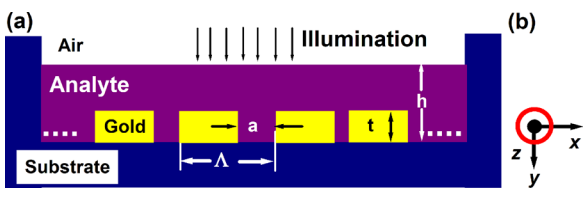

FIG. 1. (a) Schematic of the grating structure, where Λ—periodicity, a the slit width, and t—thickness, and (b) TM-polarization of the illumination.

[a)]Authors to whom correspondence should be addressed. Electronic addresses: svempati01@qub.ac.uk and tahir.awan@uog.edu.pk
[b)]S. Vempati and T. Iqbal contributed equally to this work.

simulation plane) at normal incidence (y-axis, Fig. 1(b)). The optical properties of Si and Au were adopted from Ref. 25. The reflection spectrum is obtained via finite element method from COMSOL multiphysics[26] in the presence of perfectly matched layers on top and bottom of the computational domains with periodic boundary conditions. We have used a resolution of 1 nm for the narrow regions while the whole model was meshed with maximum element size of 20 nm. The details are as follows. Maximum element size scaling factor, 1 nm; element growth rate, 1.3 nm; mesh curvature factor, 0.3; and mesh curvature cut off, 0.001 nm. The element shape was triangular (quad), which allows an accurate description of the plane wave.[27] The gradient condition increases the number of data points as the spatial distribution of the field becomes more complicated. For instance, an evanescent wave is professionally explained when a gradient in mesh resolution is used. Furthermore, the gradient mesh is useful to simulate the interaction of photons with real metal surfaces, since the skin depth and field enrichment results in a quick onset of very large field gradients over a tiny distance. The source-field and the reflection in the far-field were at a distance of 1500 nm and 1000 nm when measured from the top of the analyte, respectively. The spectra were acquired (600–900 nm) by considering the component of the Poynting vector propagating along the incident field direction at various h values (220–2200 nm). Fabry–Perot (FP)-like resonance modes are dependent on slit width and depth of the grating, which however can interfere with the Wood's anomaly (onset of the 1st order diffracted wave which propagates along the grating surface) producing other modes.[19] In the present case, the relevant parameters were optimized (results not shown here) in such a way that the FP-like resonances were suppressed in the region of spectral interest[10,19] while maximizing the absorption for surface waves. The resulting parameters were $\Lambda = 630$ nm, $a = 160$ nm, and $t = 220$ nm, and the whole structure is referred to as Λ630-a160-t220-h(220–2200) for convenience.

RESULTS AND DISCUSSION

The activation of surface modes requires either evanescent or grating coupling, where the latter introduces additional wave-vector along the parallel direction.[11,12,14,20,21] Narrow slits support TM waveguide mode propagating inside the slits in contrast to cylindrical apertures.[11,12,19–21] A metal grating surrounded by a dielectric medium supports three resonant states (RS), which can be identified in a reflection spectrum. These RS are (i) waveguide formed within the metal strips (broad band resonance, metal-insulator-metal structure),[10] similar to FP cavity mode, (ii) propagating SPPs, and (iii) involve the whole grating periodicity depending on the availability of FP cavity modes. RS (iii) are bound to the surface of the grating however, can generate a leaky mode by coupling through the slits depending on the availability of a FP-like cavity mode.[10] Essentially, for wavelengths close to Λ, the reflection minimum of 1D grating follows the dispersion relation of bound surface waves.[19,28] These surface waves become leaky for $\lambda < 2\Lambda$ where their dispersion is determined by the geometrical parameters and the finite conductivity[29] of the metal.[14,19] Note that the dispersion of the leaky surface waves is quite different from that of unperturbed surface plasmons. On the other hand, because of the asymmetry, SPP modes are excited at the input and output interfaces in addition to FP cavity modes. Importantly, coupling among FP and SPP modes can generate hybrid modes carrying the characteristics of constituents.[10,19] It is notable that the grating parameters were optimized such that the slits are in anti-resonant condition at the wavelengths in which the RS (iii) associated with the two interfaces occur (1st and 2nd order FP modes ∼1150 nm and ∼509 nm, respectively).[10,19] Also, the presence of a substrate does not significantly alter the physics of the structure, other than inducing a spectral shift of FP and plasmonic resonances.[19]

Fig. 2 shows the reflection spectra from Λ630-a160-t220-h(220–2200) grating. Due to the asymmetry,[22] the resonance modes seen in the reflection spectra are highly dependent on the contrast of RI of the (two) surrounding media (i.e., analyte and Si). For $h = 220$ nm, the analyte just fills the cavity of Au strips and shows a local minimum at ∼630 nm. As h value increases, the minimum becomes prominent and red-shifts, where the shift is governed by the effective RI. The red-shift can be calibrated against h and used to determine the thickness of the analyte.[10] However, in Ref. 10, the spectral shift of the said minimum is shown until $h = 500$ nm. Further increase in h, for example, $h \geq 800$ nm [Ref. 30], a new resonance (λ_1) feature starts to emerge and becomes prominent with increasing h. While for $h > 1000$ nm and $h > 1400$ nm, we can see the additional minima, which are referred to as λ_2 and λ_3, respectively. The resonance wavelengths λ_0, λ_1, λ_2, and λ_3 can be attributed to RS (iii), while we will see in the following that this attribution is really the case.

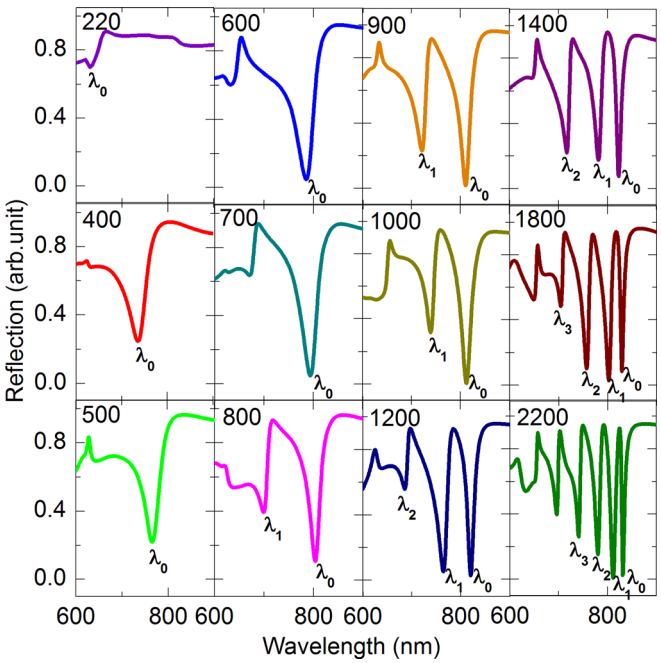

FIG. 2. Reflection spectra from Λ630-a160-t220-h(220-2200) grating. The h value is annotated on the corresponding spectrum. The surface wave resonance wavelengths are identified with λ_0, λ_1, λ_2, and λ_3 if available.

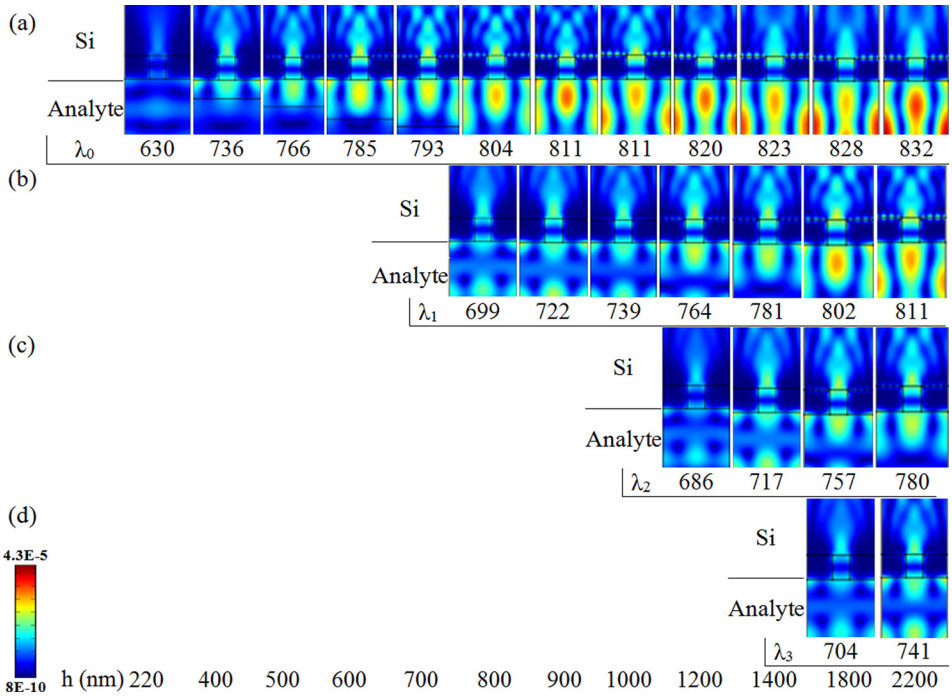

FIG. 3. False colored magnetic field plots ($630\times\sim1100\,nm^2$) from the grating Λ630-a160-t220-h(220-2200). λ_0, λ_1, λ_2, and λ_3 are the surface wave resonance wavelengths (in nm) with respect to h shown in (a)–(d), respectively. Same color scale is given for all cases.

To identify the origin of these SPP modes at the resonance wavelengths λ_0, λ_1, λ_2, and λ_3, magnetic field distributions ($|M|$) for h = 220–2200 nm were shown in Figs. 3(a)–3(d), respectively. The presence of the surface wave can be seen for all 25 cases corresponding to the minima in Fig. 2. From Fig. 3(a), it is clear that at 630 nm, $|M|$ related to the surface wave is distributed on Au/analyte interfaces, which sustains for increasing the h value. It is quite interesting to note that this behavior is similar for other sets of surface waves, *viz.*, λ_1, λ_2, and perhaps λ_3 in Figs. 3(b)–3(d), respectively. Significant changes in the effective RI induce additional (λ_1, λ_2, and λ_3) sets of surface wave modes on Au/analyte interface. As expected, all these RSs red-shift with increasing h before saturation. Since λ_1, λ_2, and λ_3 are not integer multiples of λ_0, the possibility of the former being higher order surface modes of the latter can be ruled out. On the other hand, if the contrast between the RI on either side of the grating is decreased, then the resonance wavelengths of the two interfaces become comparable. In this case, the magnitude of "asymmetry"[22] decreases and the grating can be approximated to "symmetric"[20]-type, which supports the SPPs at both the interfaces simultaneously. Under these circumstances, the SPPs on both the sides can couple through the slits, provided a FP mode is available within that wavelength range. This coupling creates two degenerate SPP modes propagating all at once on both the interfaces.[21] However, this is not the case here as we can see from Fig. 3 that the surface wave mode exists only on Au/analyte side for the given h values. In other words, this mode does not exist on both the sides at once due to the lack of coupling between the two interfaces, which is achieved by depleting the FP mode within the wavelength range of interest. To emphasize, FP mode within the slit is highly dependent on the geometry ($\lambda = 2t \times$ effective RI) of the single slit[10] although the effective RI changes with h. Having said that as the h increases further (>2200 nm), there is a possibility that the FP mode may occur (due to the change in the effective RI) and hence a coupling between the SPPs on either side may be expected. Keeping this coupling aside, it is convincing that the modes at λ_0, λ_1, λ_2, and λ_3 are in fact surface modes and exist on Au/analyte interface. Furthermore, from Fig. 3, the wavelengths listed under λ_0 and λ_1 do not spectrally shift at higher h values. This saturation-like behavior is discussed in the following.

The spectral location of the resonance wavelengths λ_0, λ_1, λ_2, and λ_3 against h were plotted in Fig. 4. The curves were individually normalized with respect to the maximum on both the axes. This double normalized plot clearly indicated that the curves do not trace each other (not shown here), which is nothing but a non-universal saturation behavior. We treat this behavior as "non-universal" by given the fact that all the modes are surface waves and expected

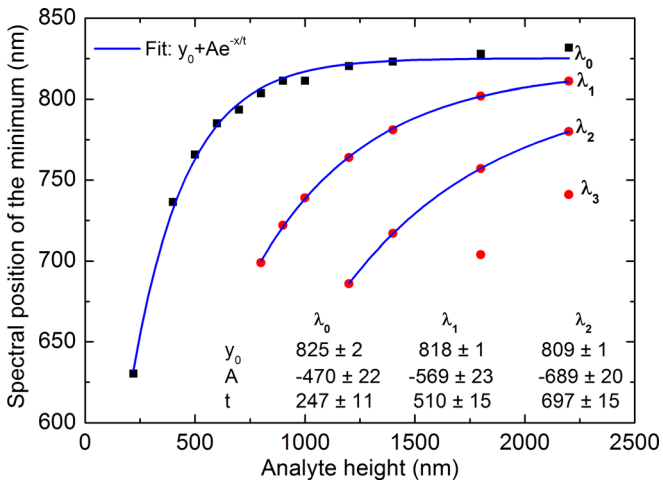

FIG. 4. Spectral position of surface wave resonance modes (λ_0, λ_1, λ_2, and λ_3) from Λ630-a160-t220-h(220-2200) with varying h values. Single exponential fit and their parameters were also shown for first three resonance modes where $R^2 \approx 0.99$ for all fittings.

to respond universally to changes in the effective RI. The saturation behavior resembles a single exponential type ($y = y_0 + A^*\exp(-x/t)$) and the fits are shown on Fig. 4 for all cases, including the fit-output. Starting with the time constants of the fits, they sharply increase, i.e., $t_0 < t_1 < t_2$, where t_0, t_1, t_2 are referred to λ_0, λ_1, and λ_2, respectively. It is interesting to note that t_1 and t_2 are nearly twice and thrice that of t_0 (within the error limits), respectively, and of course require further investigation for clear understanding of this relation. At the same time, λ_1, λ_2,and λ_3 may not be the higher order modes of λ_0. By considering the first two resonance wavelengths in each set, the differential red-shifts with respect to h are $(d\lambda/dh) \sim 0.59$, ~ 0.23, and ~ 0.09 for λ_0, λ_1, and λ_2, respectively. Apparently, $d\lambda/dh$ may approach zero for λ_i ($i > 3$) and h values exceeding 2200 nm, i.e., no red-shift with increasing h, which essentially suggests two plausible reasons. (1) No change in the effective RI with h and, (2) the surface waves become insensitive. By given the basic nature of effective RI,[31] it is possible to entangle these two complex possibilities through a logical elimination-approach. If (1) is true then λ_1, λ_2, and λ_3 would not appear and hence the possibility-(2) is the most likely factor. In what follows is the discussion on the insensitivity of the surface modes. From Fig. 4, it can be expected that for λ_1, λ_2, and λ_3, the saturation will take place, however, at relatively higher h values. Interestingly, despite being non-universal, the y_0 of λ_1, λ_2, and λ_3 will match to that of λ_0 at a certain analyte height, where the y_0 ($\sim$825 nm) is the characteristic wavelength of the present grating design. This characteristic wavelength (y_0) depends on the grating parameters, which were optimized to suppress the FP modes while supporting the surface waves within the wavelength range. Hence, for any of the surface waves, the red-shift can be expected until this value is approached. It is notable that "*insensitive*" should be referred to the context where the effective RI introduces the second set of surface waves not to the zero shift of plasmon resonance with change in effective RI. Surface wave plasmon resonance shifts with change in the effective RI.

CONCLUSIONS

It is known that the surface plasmons are quite sensitive to the changes in the RI, so is the case with surface waves on 1D asymmetric grating. These surface waves can be employed to estimate the height of analyte as well, where the changes in the effective RI are calibrated. Essentially, the resonance wavelength red-shifts with increasing h value while after a certain h value, new sets of surface waves emerge. As expected, the resonance wavelength of these new sets also red-shifts with h. Notably, the red-shift saturates exponentially in all cases however, with different time constants, i.e., the surface waves respond non-universally to the changes in the effective RI.

Although the saturation profiles were not universal, the y_0 values from the fitting may be equal to each other at much higher h values. This might be a characteristic wavelength of the present design. These modes stopped responding once the characteristic wavelength is reached, i.e., $\sim$825 nm for the present design. This wavelength depends on the grating parameters those were optimized to suppress the FP modes within the wavelength range. Also, when a mode is at the onset of the saturation (characteristic wavelength) λ_0 (λ_1), the grating starts to support λ_1 (λ_2). On the other hand, t_1 and t_2 are nearly twice and thrice that of t_0, respectively, where λ_1, λ_2, and λ_3 may be not the higher order modes of λ_0. We believe that this study not only provides new insights in designing the plasmonic sensors but also has fundamental importance in the context of behavior of plasmonic surface waves.

[1] B. L. C. Nylander and T. Lind, Sens. Actuators **3**, 79 (1982).
[2] B. Liedberg, C. Nylander, and I. Lundstrom, Sens. Actuators **4**, 299 (1983).
[3] E. Kretchmann and H. Raether, Z. Naturforsch. **23a**, 2135 (1968). Available at: http://zfn.mpdl.mpg.de/data/Reihe_A/23/ZNA-1968-23a-2135_n.pdf.
[4] B. Stein, E. Devaux, C. Genet, and T. W. Ebbesen, Appl. Phys. Lett. **104**, 251111 (2014).
[5] B. B. Zeng, Y. K. Gao, and F. J. Bartoli, Appl. Phys. Lett. **105**, 161106 (2014).
[6] J. N. Anker, W. P. Hall, O. Lyandres, N. C. Shah, J. Zhao, and R. P. V. Duyne, Nature Mater. **7**, 442 (2008).
[7] S. W. Zou, F. Q. Wang, R. S. Liang, L. P. Xiao, and M. Hu, IEEE Sens. J. **15**, 646 (2015).
[8] Y. Ding and Z. W. Liao, Physica B **464**, 51 (2015).
[9] K. Brahmachari and M. Ray, J. Appl. Phys. **117**, 083110 (2015).
[10] M. Grande, R. Marani, F. Portincasa, G. Morea, V. Petruzzelli, A. D'Orazio, V. Marrocco, D. de Ceglia, and M. A. Vincenti, Sens. Actuators, B **160**, 1056 (2011).
[11] N. Mattiucci, G. D'Aguanno, M. J. Bloemer, and A. Alu, Appl. Phys. Lett. **104**, 221113 (2014).
[12] M. A. Vincenti, M. Grande, D. de Ceglia, T. Stomeo, V. Petruzzelli, M. D. Vittorio, M. Scalora, and A. D'Orazio, Appl. Phys. Lett. **100**, 201107 (2012).
[13] H. Gao, J.-C. Yang, J. Y. Lin, A. D. Stuparu, M. H. Lee, M. Mrksich, and T. W. Odom, Nano Lett. **10**, 2549 (2010).
[14] H. Raether, *Surface Polaritons on Smooth and Rough Surfaces and on Gratings* (Springer-Verlag, Berlin, 1988).
[15] M. E. Nasir, W. Dickson, G. A. Wurtz, W. P. Wardley, and A. V. Zayats, Adv. Mater. **26**, 3532 (2014).
[16] P. C. Wu, G. Sun, W. T. Chen, K. Y. Yang, Y. W. Huang, Y. H. Chen, H. L. Huang, W. L. Hsu, H. P. Chiang, and D. P. Tsai, Appl. Phys. Lett. **105**, 033105 (2014).
[17] D. J. Sirbuly, A. Tao, M. Law, R. Fan, and P. Yang, Adv. Mater. **19**, 61 (2007).
[18] A. K. Sharma, J. Appl. Phys. **114**, 044701 (2013).
[19] D. de Ceglia, M. A. Vincenti, M. Scalora, N. Akozbek, and M. J. Bloemer, AIP Adv. **1**, 032151 (2011).
[20] D. Pacifici, H. J. Lezec, H. A. Atwater, and J. Weiner, Phys. Rev. B. **77**, 115411 (2008).
[21] M. Guillaumee, L. A. Dunbar, and R. P. Stanley, Opt. Express **19**, 4740 (2011).
[22] Asymmetry is referred to the context where the dielectric response is not symmetric on the either side of the grating.
[23] R. Marani, M. Grande, V. Marrocco, A. D'Orazio, V. Petruzzelli, M. A. Vincenti, and D. de Ceglia, Opt. Lett. **36**, 903 (2011).
[24] P. Englebienne, A. V. Hoonacker, and M. Verhas, Spectroscopy **17**, 255 (2003).
[25] E. D. Palik, *Handbook of Optical Constants of Solids* (Academic Press, San Diego, CA, 1998).
[26] Comsolmultiphysics, Version 3.5a. Available at: http://www.comsol.com/comsol-multiphysics.
[27] G. M. Ziegler, *Lectures on Polytopes*, Graduate Texts in Mathematics Vol. 152 (Springer-Verlag, Berlin, Heidelberg, New York, London, Paris, Tokyo, Hong Kong, 1995).
[28] J. Garcia-Vidal, L. Martin-Moreno, T. W. Ebbesen, and L. Kuipers, Rev. Mod. Phys. **82**, 729 (2010).
[29] E. M. Akinoglu, T. Sun, J. Gao, M. Giersig, Z. Ren, and K. Kempa, Appl. Phys. Lett. **103**, 171106 (2013).
[30] Although we have mentioned h = 800 nm as a start of the new set of surface waves, the actual signature can be evidenced even at h = 700 nm.
[31] Effective RI depends on the "wavelength" and "mode" in which the light propagates. Note that it is not just a material property, rather it depends on the whole grating design.